Thermodynamics and kinetics of moisture transport in bitumen

Ma, Lili; Varveri, Aikaterini; Jing, Ruxin; Kasbergen, Cor; Erkens, Sandra

DOI
10.1016/j.matdes.2022.111028

Publication date
2022

Document Version
Final published version

Published in
Materials and Design

Materials & Design 222 (2022) 111028

Contents lists available at ScienceDirect

Materials & Design

journal homepage: www.elsevier.com/locate/matdes

Thermodynamics and kinetics of moisture transport in bitumen

Lili Ma, Aikaterini Varveri, Ruxin Jing *, Cor Kasbergen, Sandra Erkens

Faculty of Civil Engineering and Geosciences, Delft University of Technology, Delft, Netherlands

HIGHLIGHTS

- A parameter optimization approach combined with the finite element method is proposed to study moisture transport in bitumen.
- Clustering of water molecules occurs at high relative humidity levels, accompanied by significant decrease of moisture diffusion coefficient.
- The diffusion coefficient and water cluster size of each binder type depends on the bitumen chemical and structural properties.
- The Flory-Huggins analysis of moisture isotherms reveals a feasible method to measure the bitumen solubility parameter.

GRAPHICAL ABSTRACT

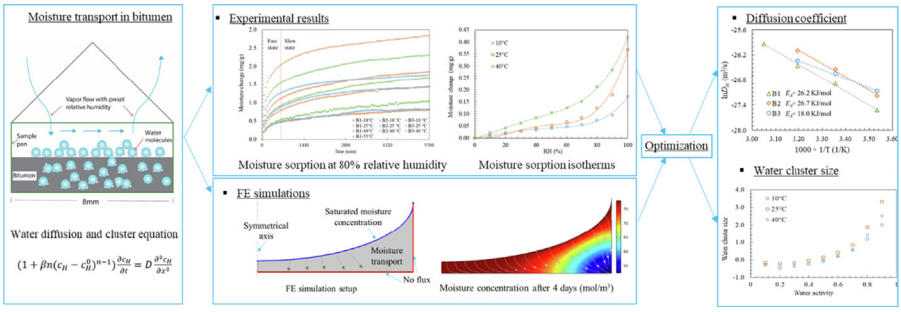

ARTICLE INFO

Article history:
Received 16 March 2022
Revised 4 July 2022
Accepted 2 August 2022
Available online 5 August 2022

Keywords:
Bitumen
Moisture
Transport
Optimization
Clustering

ABSTRACT

Moisture in bitumen and at the bitumen-aggregate interface affects the cohesive and adhesive properties of asphalt mixtures, which are critical for the service performance and durability of pavements. This paper aims to investigate the kinetics and thermodynamics of moisture transport in bitumen at various temperatures and relative humidity for different bitumen types. Transport models are introduced to study the moisture transport mechanisms. A parameter optimization approach combined with the finite element method is applied to simulate moisture transport behavior. Results show salient sorption increase at higher relative humidity levels (more than 70%), indicating the occurrence of clustering of water molecules in bitumen, which can lead to a significant decrease of the diffusion coefficient. Transport models show great quality in simulating experimental results, in which the S-Cluster model provides a detailed explanation of the moisture transport mechanisms and describes better the performance at high sorption levels. The diffusion coefficient, cluster size and activation energy were determined and were found to be linked to the bitumen chemical and structural properties. The transport kinetics and thermodynamics are expected to contribute to a comprehensive understanding of moisture transport behavior in bitumen and further of pavement moisture damage at complex and interacting environmental conditions.

1. Introduction

Bitumen is a widely-used binder for paving roads and waterproof applications especially for roofing. Climatic factors have a significant influence on bituminous mixtures including moisture, temperature, UV radiation etc. For example, UV light can accelerate

* Corresponding author.
E-mail address: r.jing@tudelft.nl (R. Jing).

https://doi.org/10.1016/j.matdes.2022.111028
0264-1275/

the ageing process and result in an increase of bitumen stiffness and brittleness [1]. Moreover, temperature controls the viscoelastic response of bitumen, whereas moisture can significantly affect the mechanical properties of bitumen and bituminous mixtures [2]. The pavement failure in the presence of moisture occurs mainly due to the loss of bitumen cohesion and of adhesion at the bitumen-filler (in mastic systems) or bitumen/mastic-aggregate interfaces. The failure mode changes from cohesive to adhesive with increasing moisture concentration and decreasing temperature [3,4]. The cohesive energy density inside bitumen decreases due to the volume increase as moisture diffuses into the bulk [5], and results to decreased cohesion strength of bitumen [6]. Adhesion loss may be more serious compared to cohesion failure at moist conditions [7] and adhesion strength at the mastic-aggregate interface can be assumed as a function of moisture content [8].

Moisture transport in bituminous mixtures involves convective flow in the void network, diffusion within the bulk bitumen/mastic and accumulation at the mastic-aggregate interface. Diffusion is one of the crucial mechanisms leading to moisture damage, and can be defined as the molecular motion generated by the moisture concentration gradient. Sorption refers to the thermodynamic equilibrium state of moisture transport, including surface adsorption and bulk absorption. Diffusion describes the kinetics of bulk absorption. Two factors are crucial in the processes of moisture sorption and transport in bituminous materials: the rate of moisture diffusion and the equilibrium moisture content (solubility) [9]. Diffusion kinetics are generally characterized by Fick's law [10]. However, moisture diffusion in bitumen may display non-Fickian behavior. The chemical composition and microstructure of the bituminous matrix can strongly influence moisture sorption and transport mechanisms, leading to deviation from Fick's law [11]. When absorbed moisture concentration is relatively high, bonds amongst the water molecules (hydrogen bonding) and bonds between the water molecules and the polar groups of materials can be created, accompanied by a reduction of the diffusion coefficient [12]. The dual-mode model, the Langmuir-diffusion model and the time-variation model have been developed to address the non-Fickian behavior of moisture transport in bituminous materials [13–15]. Different materials also show different adsorption kinetics, for example following first-order adsorption rate or second-order adsorption rate laws, based on the surface characteristics and the interaction between adsorbate and adsorbent [16].

Except for the kinetic surface adsorption and bulk diffusion process, the equilibrium adsorption and absorption isotherms of moisture are also of significant importance for moisture damage in bituminous materials [9]. The Langmuir monolayer isotherm and the Brunauer–Emmet–Teller (BET) multilayer isotherm are commonly utilized to describe the adsorption phenomena. Other models, i.e. the Guggenheim–Anderson–de Boer (GAB) model, Dubinin-Radushkevich (DR) model, etc., have been introduced to explain the multilayer adsorption of moisture at high relative humidity [17]. Moisture absorption in materials containing polar groups, such as bitumen, can exhibit a clustering behaviour at high concentration as the water molecules do not only bond with water molecules through hydrogen bonds, but associate with the hydrophilic sites or polar groups of the materials [5,18,19]. Moreover, the saturated moisture concentration (or moisture solubility) is as a function of relative humidity; at low relative humidity level, the solubility can be expressed based on Henry's law, whereas at high relative humidity the Flory-Huggins solubility and other more complex theories can be considered [20].

Limited studies have been done to investigate the moisture sorption and transport behavior at bitumen scale. Spectroscopic methods, such as the Fourier transform infrared-attenuated total reflectance (FTIR-ATR) [11] and gravimetric methods [9] were used to measure moisture diffusion in bitumen. FTIR-ATR can detect the overall moisture content in bitumen films, that were subjected to continuous water conditioning, by calculating the area from 3000 to 3800 cm^{-1} that characterizes the presence of moisture. Results show that moisture sorption–desorption cycles increase the moisture diffusion coefficient in bitumen, which could be attributed to microstructural changes after cyclic moisture exposure as shown in atomic force microscopy (AFM) images [21]. The gravimetric methods monitor the mass change with time at sub-microgram resolution. Other methods, such as the electrochemical impedance spectroscopy (EIS) were used to measure moisture diffusion under the assumption that the capacitance is correlated with moisture content. The diffusion coefficient values determined in the various studies show considerable deviations [22]. Two deciding factors are responsible for the big differences of moisture diffusion coefficient from experiments: the systematic errors of measuring protocols and the quality of theoretical transport models. Aforementioned transport models including the dual-mode model [11] and the Langmuir diffusion model [23] overall describe two moisture transport modes: free mode and immobilized or less mobile mode due to the attraction of water molecules to the functional groups in bitumen or the clustering of water molecules.

This paper aims to study the diffusion coefficient and solubility of moisture in bitumen at various combinations of temperature and relative humidity. Transport models for describing the thermodynamic equilibrium sorption and kinetic transport of moisture at the surface and in the bulk of bitumen were introduced and compared to study the transport mechanisms and predict moisture behavior in bitumen. A parameter optimization method was applied to solve the transport models. The moisture sorption isotherms, transport kinetics and the water clustering mechanism were further discussed.

2. Materials and methods

2.1. Sample preparation

In this study, two 70/100 penetration grade bituminous binders supplied from Vitol and Total Energies, and one styrene–butadiene–styrene (SBS) modified bitumen were used for performing gravimetric tests to investigate moisture transport behavior in bitumen. The bitumens are named as B1, B2 and B3, respectively. The SBS modified bitumen was prepared by using the Vitol 70/100 penetration grade bitumen as the base binder and adding 4 wt% (by bitumen weight) Kraton D1102 SBS, which is a linear block copolymer with 28.5 % styrene, provided by Kraton Corporation. For the preparation of the samples, first a small amount of bitumen was cut from the stored bitumen and weighed in a high-precision scale to a weight of 40 ± 1 mg; subsequently the bitumen was placed in an aluminum pan with 2.75 mm height and 8 mm diameter and then heated at 160 °C for approximately 60 s to allow bitumen to spread on the bottom of sample pan and create a thin film (Fig. 1(a)).

2.2. Experimental procedure

The Dynamic Vapor Sorption (DVS) system from Surface Measurement Systems (SMS) ltd. was used for the gravimetric tests with a precise control and measurement of temperature, relative humidity (RH) and mass change. The system measures the change of sample mass with a resolution of 0.1 μg. Relative humidity is controlled by mixing and adjusting the ratios of saturated water vapor and pure dry carrying gas. A vapor stream at a specified relative humidity is purged into the sample chamber with a recom-

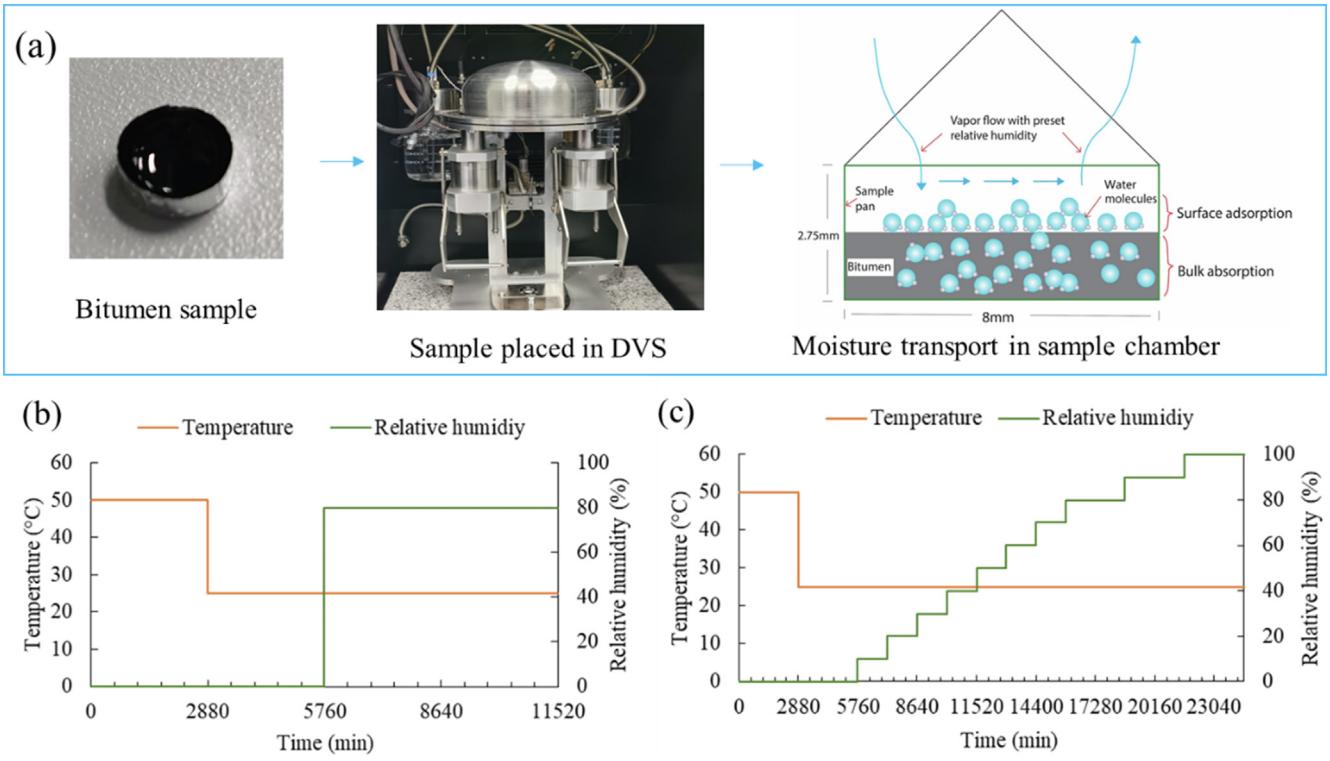

Fig. 1. (a) Moisture transport measurement procedures and DVS tests for moisture transport via (b) constant RH and (c) multi-step RH methods.

mended flow rate of 200 sccm (cm^3/min). It is suggested that such flow rate ensures instantaneous supplement of moisture concentration loss above sample surface due to sorption of bitumen, thus providing a constant boundary condition. In addition, such gas flow rate could accelerate the transport process with little effect on the isotherm results [24,25]. In this study, the air was used as carrying gas to replicate the actual situation in the atmosphere. The effect of oxidative ageing on the sample mass change and transport behavior was neglected considering the low temperatures (10 °C to 40 °C) and short test periods (8 to 17 days).

To determine the time at which the sample has reached moisture sorption equilibrium, often a dm/dt (change in mass within a unit time) criterion is adopted, in which equilibrium is defined when limited change in mass occurs for a specified time period. However, for the moisture transport tests, the mass change rate in the bitumen samples was smaller than the dm/dt value caused by the instrument balance fluctuation in most cases. With the dm/dt method, the test will never be completed due to the dm/dt criterion but because of the achievement of the specified maximum step time. Therefore the time-based method was directly used for moisture transport tests. A series of trial tests were performed to define the duration of the humidity steps so as to ensure that samples would reach equilibrium. On the basis of the trial tests, a drying step of two (2) days at elevated temperature (55 °C) was applied to remove pre-existing moisture in bitumen samples and to balance the effects of any discrepancies during sample preparation, as well as the subsequent 2 days at testing temperatures to continue drying and provide a steady temperature environment for further vapor loading.

Two test methods were applied to study the moisture transport behavior, namely the constant RH and the multi-step RH tests (Fig. 1(b) and (c)). The constant RH method consisted of two steps i.e. 4-day drying and 4-day RH loading at 80 %, which is approximately the average relative humidity in Netherlands. The binders (B1, B2 and B3) were tested using constant RH method at the temperatures of 10 °C, 25 °C, 40 °C (and 55 °C exclusively for B1) to investigate the effect of temperature on the moisture transport kinetics of three types of bitumen. For the multi-step RH protocol, after the drying step, RH was applied from 0 % to 100 % with a step size of 10 % [26]. The moisture transport of B1 at three temperatures (10 °C, 25 °C, 40 °C) was implemented following the multi-step RH protocol to measure the moisture sorption isotherms at different temperatures.

2.3. Surface area measurement

Aluminum has high surface energy and the bitumen in an aluminum pan is likely to flow and adhere to the side walls forming a upward concave surface when heating as seen in Fig. 2. The Digital Microscope VHX-7000 with 100x lens from Keyence was used to characterize the sample surface. Bitumen, as a black petroleum residue, absorbs most of the lights from LED light source, making it difficult to measure the surface structure. Therefore, the hydrated lime filler Wigro 60 K was spread on the sample surface to create a thin grey film. The filler has a percentage passing of 83 % for the sieve size of 0.063 mm, much smaller than the thickness of bitumen film, thus having limited effect on the measured results. The concave surface curve of half a 2D cross section (assuming symmetrical cross section over the center) was fitted using the ellipse equation. Three samples with same preparation procedures were measured to determine the average height of the ellipse (h_e in Fig. 2). The bitumen sample surface thus composes of a cylinder with the height of h_c and a cylinder with height of h_e subtracted by a ellipsoid having the same height of h_e.

2.4. Modeling methodology

The transport of moisture from environment to bitumen is considered to occur in two stages. Specifically, it is assumed that water molecules are first adsorbed on the bitumen surface establishing a

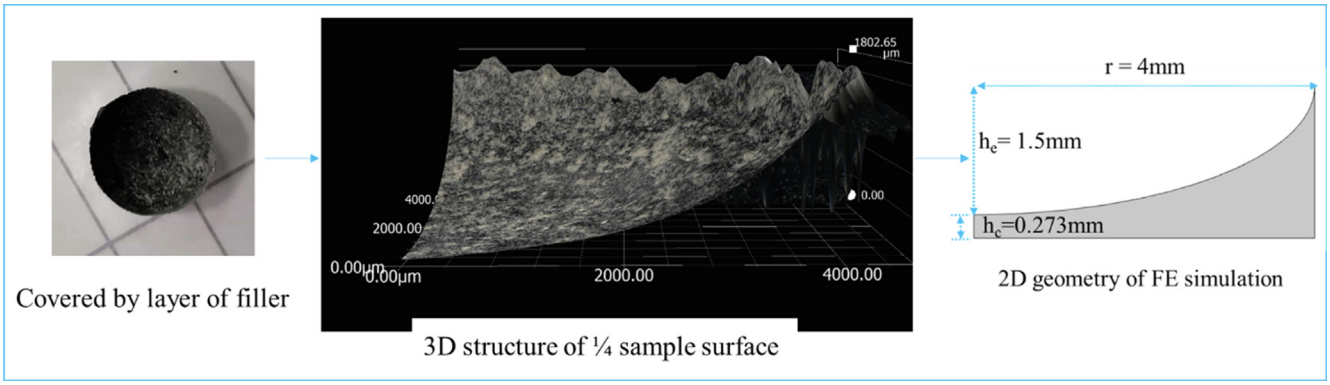

Fig. 2. Microscopy measurement of bitumen surface and derived 2D geometry for FE simulations.

constant surface water concentration. These adsorbed molecules then diffuse into bulk bitumen due to the presence of a concentration gradient. Adsorption is theoretically much faster than bulk diffusion, considering that the adsorption is a surface phenomenon with a wider area exposed to the adsorbate while absorption is a bulk behavior facing more resistance of the internal interaction forces [27,28].

The pseudo-first order (PFO) model proposed by Lagergren is widely used to describe the adsorption kinetics [29], suggesting an adsorption rate equation following the first order relationship, which can also be described as the linear driving force model [30]:

$$\frac{ds}{dt} = \alpha(s_m - s) \tag{1}$$

where s denotes the adsorbed moles of gas per gram and s_m is the maximum adsorbed value, and α is the adsorption rate constant.

From equation (2), assuming the initial value of s is 0, we can get the solution of the PFO model:

$$s = s_m(1 - e^{-\alpha t}) \tag{2}$$

Bulk absorption refers to the thermodynamic equilibrium state of diffusion process when there are no macro voids. The diffusion process is generally described by Fick's law [31]. Fick's first law illustrates that the diffusion flux is proportional to the concentration and Fick's second law predicts how the concentration changes with time. When the diffusion coefficient is independent of concentration, Fick's second law is defined as:

$$\frac{\partial c}{\partial t} = D\nabla^2 c \tag{3}$$

where D is the diffusion coefficient, t is the time and c is the concentration of diffusing species.

Non-Fickian diffusion can take place when the diffusing gas/vapor shows polarity such as water and the absorbent contains polar groups such as bitumen. The dual-phase diffusion model has been proposed to describe the moisture transport behavior [32]. This model assumes that diffused molecules have two states: one state describes molecules that are free to diffuse and the other state refers to molecules fixed to certain sites or having much slower diffusion rate. Both states still follow Fick's law but with two different diffusion coefficients D_1 and D_2 [12].

$$\frac{\partial c_1}{\partial t} = D_1\nabla^2 c_1 \tag{4}$$

$$\frac{\partial c_2}{\partial t} = D_2\nabla^2 c_2 \tag{5}$$

$$c_{moi} = c_1 + c_2 \tag{6}$$

where c_1 is the free water concentration, c_2 is the bound water concentration, and c_{moi} is the whole water concentration.

Besides, in the cluster model developed by Park [26,33], at lower partial pressure, the water solubility is proportional to its partial pressure as indicated by Henry's law. As the water partial pressure increases, the bulk water concentration is quite high, thus causing the binding of a certain number of water molecules with each other or with functional groups of bitumen through hydrogen bonds:

$$n\mathrm{H_2O} \rightleftharpoons (\mathrm{H_2O})_n \tag{7}$$

where n represents the water number in a cluster.

The water concentration in the cluster mode can be described according to the following equation:

$$c_{cu} = K_c(k_d P)^n/n \tag{8}$$

where, K_c is the equilibrium constant for the clustering reaction, k_d is the Henry's law solubility coefficient, P is the water partial pressure, and $k_d P$ is the water concentration in Henry's mode. The equation can be further converted to:

$$c_{cu} = \beta\mathscr{H}(c_H, c_H^0)(c_H - c_H^0)^n \tag{9}$$

where c_{cu} is the water concentration in clustering mode, c_H is the concentration in Henry's mode, c_H^0 is the threshold of clustering, β is the clustering coefficient, $\mathscr{H}$ is the Heaviside step function and n is the average number of water molecules in an agglomeration.

The overall bulk concentration is composed of the water concentration in Henry's mode and in clustering mode:

$$\frac{\partial c_b}{\partial t} = \frac{\partial c_H + \partial c_{cu}}{\partial t} = D\frac{\partial^2 c_H}{\partial x^2} \tag{10}$$

where c_b is bulk water concentration, D is the Henry's diffusion coefficient. The water in clustering mode is considered not participating in the diffusion process.

According to equation (8), the time differential of clustering concentration is:

$$\frac{\partial c_{cu}}{\partial t} = \beta n\left(c_H - c_H^0\right)^{n-1}\frac{\partial c_H}{\partial t} \tag{11}$$

Therefore the diffusion kinetics is defined by:

$$\left(1 + \beta n\left(c_H - c_H^0\right)^{n-1}\right)\frac{\partial c_H}{\partial t} = D\frac{\partial^2 c_H}{\partial x^2} \tag{12}$$

From equation (10), the pseudo diffusion coefficient can be defined as:

$$D_{pse} = \frac{D}{(1 + \beta n(c_H - c_H^0)^{n-1})} \quad (13)$$

To study the moisture transport mechanisms and characterize the moisture transport kinetics of bitumen including surface adsorption and bulk absorption three models, namely the S-Fick model, the Dual model and the S-Cluster model, were proposed and compared based on their ability to simulate the water transport behavior in bitumen. Specifically, in the S-Fick model, surface adsorption is represented by the pseudo first-order equation and the bulk adsorption follows Fick's law of diffusion. Four parameters are to be determined including the maximum surface adsorption mass s_{m-sf}, the adsorption rate constant α_{sf}, the saturated bulk absorption concentration c_{sat-sf} and the bulk diffusion coefficient D_{sf}. In the Dual model, it is assumed that there are two water transport modes, which both follow Fick's law with specific diffusion coefficients, hence with four unknown parameters, i.e. the saturated moisture concentration c_1 and the diffusion coefficient D_1 of the first transport mode, and the saturated moisture concentration c_2 and the diffusion coefficient D_2 of the second transport mode. In the S-Cluster model, the pseudo first-order equation is used for surface adsorption, whereas bulk absorption is described by the water cluster model, where the threshold of clustering c_H^0, the clustering coefficient β, the average number of water molecules n in a agglomeration, the maximum surface adsorption mass s_{m-sc}, the adsorption rate constant α_{sc}, the saturated bulk absorption concentration c_{sat-sc} and the Henry's bulk diffusion coefficient D_{sc} are undetermined parameters.

2.5. Model solutions

The finite element (FE) method was used to simulate the moisture transport behavior in bitumen through COMSOL Multiphysics. The symmetrical two-dimensional geometry of the bitumen film was modelled based on the microscope results of the DVS samples (as shown in Fig. 2). The triangular element was utilized to mesh the geometry. For the FE simulations, no flux was specified for all boundaries, except for the surface, and the initial water concentration of the bitumen was assumed to be zero. The surface water concentration (namely the adsorbed water concentration) was set to be constant for the bulk diffusion process, considering the much faster equilibrium of surface adsorption. The three transport models were then performed in the simulations, respectively. Providing the initial guesses of the unknown model parameters, the overall mass change with time was simulated by spatial integration of moisture concentration in bitumen. Subsequently, the unknown parameters were optimized by fitting the numerical solution (simulated mass change) to the experimental data obtained from the DVS tests.

Two fundamental parts of an optimization problem are the control variables and the objective functions. In this work, the control variables are unknown parameters in the transport models as summarized in Table 1. The objective function is defined by the global least-squares objective function (Q):

$$Q = \sum_t \left(s + M \iiint c_b - m_{lab}\right)^2 \quad (14)$$

where t is the vapor loading time, s represents surface adsorption mass,M is the molar mass of water, c_b is the bulk moisture concentration and m_{lab} indicates the experimental mass change. The optimization process aims to determine the values of the control variables that minimize the objective function, i.e. the difference between simulated and experimental results. The objective function has vast sensitivity to different parameter changes considering the magnitude difference of initial parameter values and parameter bounds. Prior to the optimization, a scaling transformation is applied to all parameters to ascertain similar magnitude of values.

For the inverse problem (determining the values of a set of parameters providing simulated data which best match the measured data), in this case a non-linear inverse problem, an optimization searching method may be trapped in different local optima depending on the chosen initial estimations (seed values). It is therefore indispensable to give good initial guesses for the parameter optimization procedures. The Monte Carlo (MC) method, the Bound Optimization by Quadratic Approximation (BOBYQA) method and sensitivity analysis were combined to determine the unknown parameters in the moisture transport models as shown in Fig. 3. The Monte Carlo Solver searches randomly the data points from the uniform distribution inside the range of values specified by the parameter bounds. The solver can find several local minima inside the specific parameter intervals (if they exist). In order to find all possible local minima with high accuracy, the parameter values should be in a wide range and the sampling point density should be high, requiring much longer computation times. The BOBYQA method iteratively approximates the objective function by a quadratic model [34], thus obtaining a faster convergence rate. Instead of using MC to find more accurate values, BOBYQA method was further applied to optimize the parameter values. To conduct the parameter optimization, initial parameter values and wide parameter bounds (10 to 100 times of initial value) were determined for MC, as shown in Table 1, that had a relatively sparse data point distribution, which considered the physical meaning of each parameter on the basis of published data from literature and experimental results [22]. After obtaining optimized results from the MC process, several parameter sets with lower objective error and appreciable difference of parameter values were chosen as initial guesses for BOBYQA optimization. The output parameters from BOBYQA optimization were used again as input to perform the BOBYQA optimization. This iteration was executed until a difference of less than 2 % in the objective function and the control variables was observed; then the optimization was assumed to reach convergence and the final optimized parameter values could be obtained.

3. Results and discussions

3.1. Moisture transport models and solutions

3.1.1. Model optimization

To study the moisture transport mechanism and back-calculate the moisture transport parameters including diffusion coefficient, surface adsorption, bulk solubility etc., three models have been proposed and solved using a multi-optimization method. The objective function of various parameter sets and the corresponding objective contours are shown in Fig. 4(a). MC calculates the objective function at mesh points over designated ranges. The darkest green area implies the parameter value ranges with a lower objective error, about 95 ~ 100 mol/m^3 for c_2 and 5E-13 ~ 1.2E-12 for D_2. The parameter ranges obtained from the MC results are still relatively high even after 10,000 points evaluation. The aforementioned BOBYQA method attempts faster parameter improvement based on a quadratic approximation model in the trust region with radius of 0.2 (relative to parameter value). The objective function of BOBYQA method shows a rapid convergence in 400 evaluation steps (Fig. 4(b)). In this case, after twice iteration evaluations, the lowest objective error is acquired based on the fact that an extra iteration shows the same or inversely higher objective error.

The optimized simulation results of the three moisture transport models are illustrated in Fig. 5, together with the results of

Table 1
Overview transport kinetics models parameters.

Model	Parameter	Symbol	Unit	MC range (min, max)
S-Fick	Surface adsorption rate constant	α_{sf}	1/s	0.05, 0.5
	Equilibrium surface adsorption mass	s_{m-sf}	kg	1E-9, 1E-8
	Bulk diffusion coefficient of moisture in bitumen	D_{sf}	m^2/s	1E-14, 1E-11
	Saturated bulk absorption concentration of moisture	c_{sat-sf}	mol/m^3	40, 120
Dual	Diffusion coefficient of first transport mode	D_1	m^2/s	1E-12, 1E-10
	Diffusion coefficient of second transport mode	D_2	m^2/s	1E-14, 1E-11
	Saturated moisture concentration of first transport mode	c_1	mol/m^3	20, 100
	Saturated moisture concentration of second transport mode	c_2	mol/m^3	40, 120
S-Cluster	Surface adsorption rate constant	α_{sc}	1/s	0.001, 0.1
	Equilibrium surface adsorption mass	s_{m-sc}	kg	1E-9, 1E-8
	Number of water molecules in a cluster	n	/	1, 3
	Clustering coefficient	β	/	0.1, 5
	Threshold moisture concentration when cluster starts	c_H^0	mol/m^3	20, 100
	Henry's bulk diffusion coefficient of moisture in bitumen	D_{sc}	m^2/s	1E-14, 1E-11
	Saturated bulk absorption concentration of moisture	c_{sat-sc}	mol/m^3	40, 120

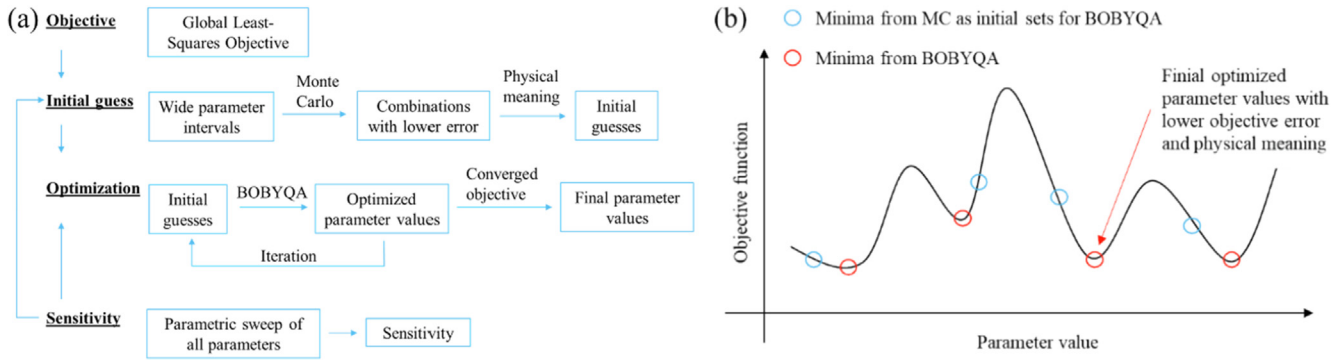

Fig. 3. Parameter optimization: (a) Flow chart of parameter determination protocol, (b) Parameter optimization results with multiple local minima.

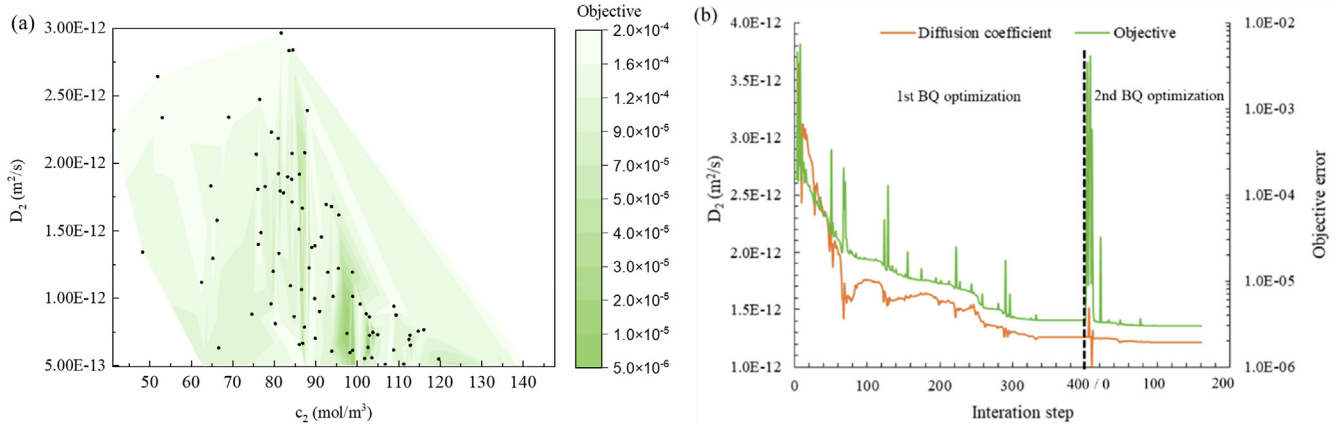

Fig. 4. Optimization solution procedures of the Dual model for B3 at 25 °C and 80 % RH: (a) Objective error contour after 10,000 MC model evaluations; black symbols are parameter values with objective smaller than 2E-04; only c_2 and D_2 are shown. (b) Diffusion coefficient convergence process with two BOBYQA iterations: the 2nd iteration step used the final result from 1st BOBYQA optimization as initial parameter values.

the classic Fick's law model. Apparently, Fick's law cannot describe well the moisture transport behavior in bitumen. The three models proposed in this work, i.e. the S-Fick, Dual and S-Cluster models, show extremely high prediction quality. To further evaluate the model performance with optimized parameters three metrics are utilized. The root mean square error (RMSD) describes the residual amount of simulation compared to experimental results:

$$RMSD = \sqrt{\frac{\sum_{i=1}^{N}\left(y_{i\_test} - y_{i\_model}\right)^2}{N}} \tag{15}$$

where N is the number of data points, y_{i_test} is the test observation value, y_{i_model} is the model estimated value. The coefficient of determination (R^2) indicates the correlation between modelled results and experiment data:

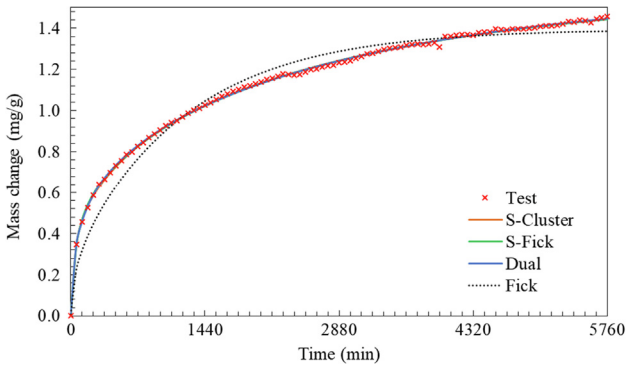

Fig. 5. Comparison of the proposed moisture transport models results with the classic Fick's law results (denoted as Fick) for B1 at 25 °C and 80 % RH.

$$R^2 = 1 - \frac{RSS}{TSS} \tag{16}$$

where $RSS = \sum_{i=1}^{N}(y_{i\_test} - y_{i\_model})^2$, $TSS = \sum_{i=1}^{N}(y_{i\_test} - \bar{y}_{i\_test})^2$. R^2 is likely to increase with an increase of the variable amount in a model. The adjusted R^2 with extra consideration of the number of parameters in a model would allow us to compare models with different numbers of independent variables [35].

$$R^2_{\text{adjusted}} = 1 - \frac{(1-R^2)(N-1)}{N-k-1} \tag{17}$$

where k is the number of variables in the model. Metrics of three models are reported in Table 2. The R^2 and R^2_{adjusted}, with values close to 1, demonstrate the great experiment-fitting capability of the three models for bitumen at various temperatures (Fig. 6(a)). The Dual model is relatively better than the S-Fick model in simulating water transport kinetics with lower RMSE for most cases. The S-Fick and Dual models have slightly lower performance at higher temperatures, especially at the transition point from fast to slow state diffusion (Fig. 6). At 55 °C, the RMSE values for the S-Fick, Dual and S-Cluster models are 1.0E-3, 9.0E-4 and 3.1E-4 respectively indicating the superior performance of the S-Cluster model at higher temperatures where increased water sorption occurs.

3.1.2. Sensitivity analysis

Analysis was performed to investigate the sensitivity of the model results with respect to changing parameters of the moisture transport models. The effects of changing values on model outputs were evaluated individually for all parameters and locally for chosen points [36]. To evaluate the sensitivity of the target parameter, all other parameters are fixed to the reference values, which are selected from the optimized parameter value sets. The local sensitivity behavior is dependent on the choice of the reference parameter values, which should be discussed with caution. The target parameter change ranges from 0.1 to 2 or to 10 (dependent on parameters) times the reference value.

The objective function dependence on parameter changes is shown in Fig. 7. For the S-Fick model, D_{sf}, c_{sat-sf}, and s_{m-sf} show similar effects on the objective function, while α has less impact on the model outputs, which indicates more difficulty in finding the specific value of α. All parameters acquire the minima at the point of the reference values, suggesting a well-optimized parameter value sets. There are seven unknown parameters in the S-Cluster model, among which s_{m-sc}, n, D_{sc}, c_{sat-sc},c^0_H have high sensitivity and β, α are less sensitive. The unsymmetrical sensitivity with respect to the minima axis, especially for n, β, α and c^0_H, proposes extra attention for optimization procedures.

3.1.3. Sources of uncertainty in moisture sorption results

Three main factors were identified in this work that can cause uncertainties in the moisture sorption results, namely the inherent balance drift of DVS, the measurement stability and the sample properties. DVS has an inherent balance drift (measured continuous mass increase or decrease with time when no actual mass change occurs), whose direction is independent of temperature and other environmental conditions. The balance drift was characterized by measuring the mass change of empty sample pans using the constant RH method at test temperatures (10 °C, 25 °C, 40 °C). The calibrated balance drift of DVS is ± 0.002 mg/4 days at all test temperatures. The moisture sorption mass in the constant RH test results is ca. 0.03 ~ 0.1 mg (dependent on temperature and bitumen type), suggesting an systematic error limit of 2.0 % ~ 6.3 % due to the balance drift. The sample loading process with sample contamination and equipment contact and the surrounding inference are specified as the measurement stability and could also affect the measured moisture mass change of the DVS. What's more, bitumen samples have different sample mass and film thickness. Specifically, the bitumen sample mass is controlled in the range of 40 ± 1 mg and the measured h_e height is in the range of 1.3 mm ~ 1.7 mm.

To examine how the repeatability of moisture sorption tests is affected by measurement stability and sample properties, three B1 samples were measured at 25 °C following the same preparation and testing procedures. Any contaminations such as dust in the sample pan and external interference could have noticeable effect on moisture sorption, especially on the initial state when contamination adsorption occurs, and the working conditions of DVS equipment change (loading relative humidity). It can also be seen from Fig. 8(a) and (b) that three samples show big difference at initial stage and converge at the end of the curve shape at later

Table 2
Evaluation of moisture transport models.

Metrics		RMSE			R2			R2-adjusted		
Bitumen types	Models	B1	B2	B3	B1	B2	B3	B1	B2	B3
10 °C	S-Fick	4.10E-04	6.80E-04	6.40E-04	0.997	0.989	0.995	0.996	0.988	0.994
	Dual	3.50E-04	6.80E-04	6.50E-04	0.997	0.989	0.995	0.996	0.988	0.994
	S-Cluster	3.90E-04	6.90E-04	6.40E-04	0.996	0.988	0.995	0.995	0.987	0.994
25 °C	S-Fick	3.30E-04	2.70E-04	3.00E-04	0.999	0.999	0.999	0.999	0.999	0.999
	Dual	3.20E-04	2.50E-04	2.30E-04	0.999	1.000	1.000	0.999	0.999	1.000
	S-Cluster	3.10E-04	2.80E-04	2.70E-04	0.999	0.999	1.000	0.999	0.999	0.999
40 °C	S-Fick	4.80E-04	6.30E-04	4.90E-04	0.999	0.996	0.999	0.999	0.996	0.999
	Dual	3.10E-04	4.30E-04	4.30E-04	0.999	0.998	0.999	0.999	0.998	0.999
	S-Cluster	3.60E-04	4.00E-04	4.70E-04	0.999	0.999	0.999	0.999	0.999	0.999
55 °C	S-Fick	1.00E-03	/	/	0.996	/	/	0.996	/	/
	Dual	9.02E-04	/	/	0.997	/	/	0.997	/	/
	S-Cluster	3.06E-04	/	/	1.000	/	/	1.000	/	/

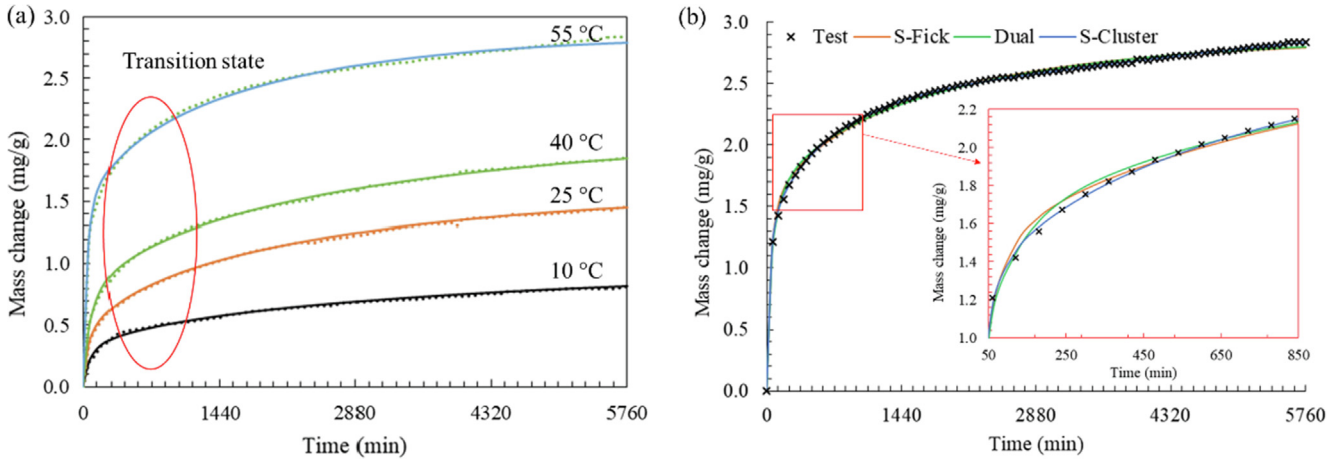

Fig. 6. (a) Comparison between the experimental results (dotted lines) and the simulated results (solid line) of moisture sorption for B1 at 80 % using S-Fick model; (b) Comparison the experiment-fitting performance of three models at 55 °C for B1 at 80 %.

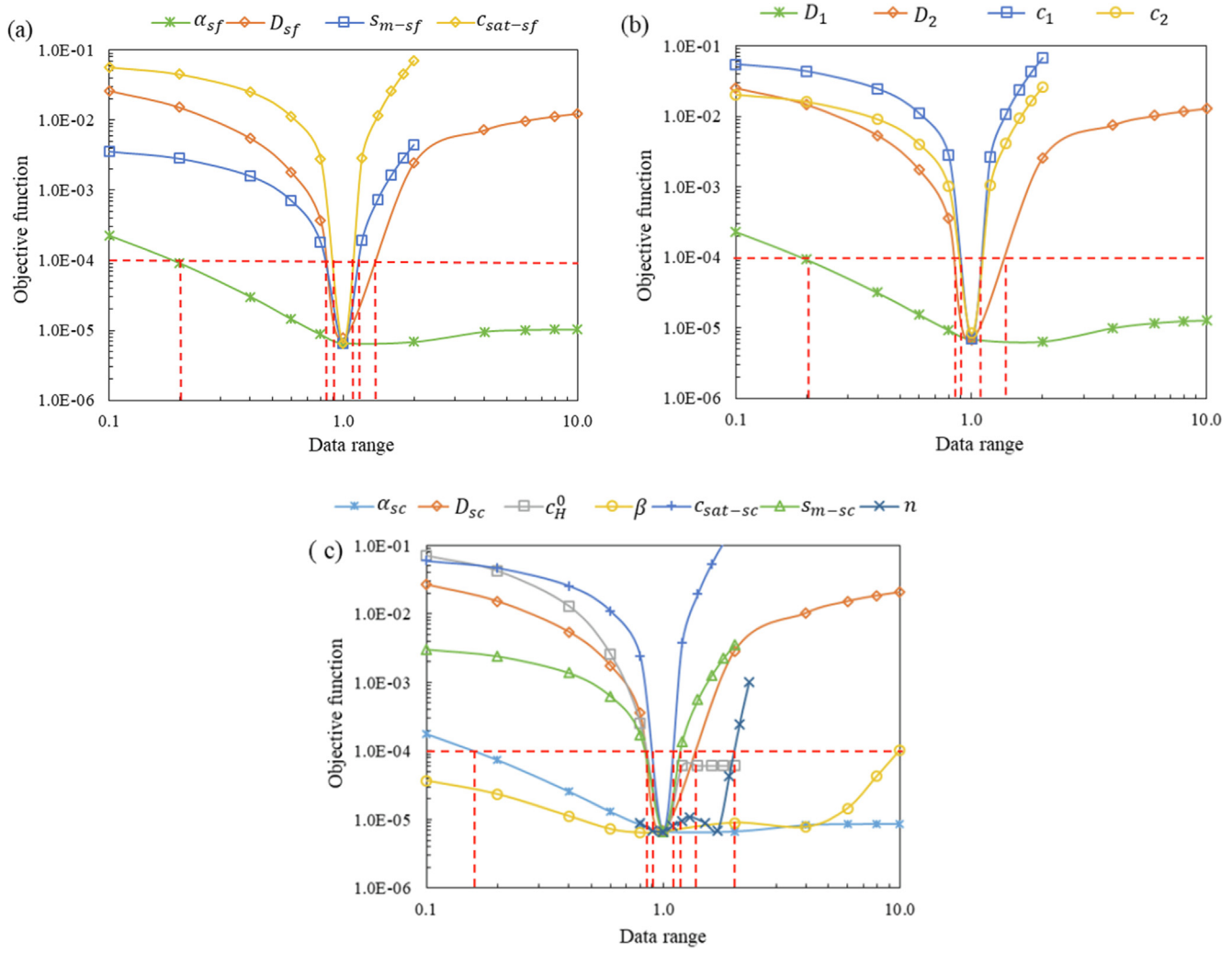

Fig. 7. Parameter sensitivity analysis of (a) S-Fick model, (b) Dual model and (c) S-Cluster models using reference parameter values from the optimized results of sample B1 at 25 °C and 80 % RH.

time. Therefore the surface adsorption is excluded using the S-Cluster model and the repeatability of bulk absorption is also determined. The relative errors (standard deviation / mean value) of the measured equilibrium sorption (adsorption and absorption) and the measured equilibrium absorption at 25 °C are approximately 15.3 % and 4.3 %, respectively. The 4.3 % deviation from

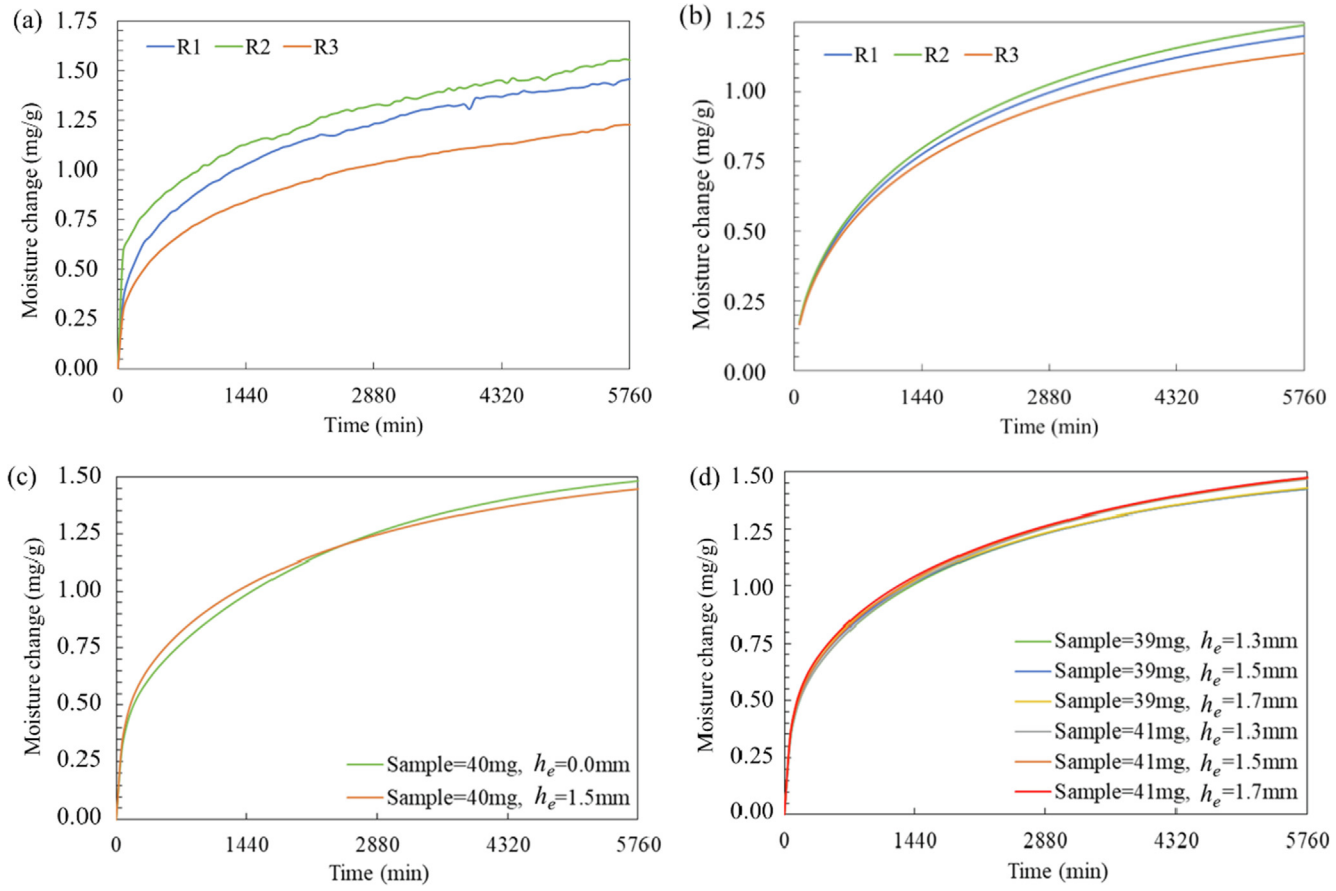

Fig. 8. (a) Moisture sorption curves for three replicate samples (R1, R2, *R3*) of bitumen B1 at 25 °C; (b) Moisture bulk absorption curves derived from the total sorption curves using the S-Cluster model for the three replicate samples; (c) The effect of bitumen film shape on moisture sorption for B1 at 25 °C using the S-Cluster model; (d) The effect of sample mass and ellipsoid height on moisture sorption for B1 at 25 °C using the S-Cluster model. The model parameter values are the same for all cases in (c) and (d), except for the sample mass and ellipsoid height.

average sorption generates an objective error of ca. 1E-4. As shown in Fig. 7, for the maximum surface adsorption, bulk solubility and diffusion coefficient from three models, this deviation of measured sorption mass could lead to a parameter uncertainty of ± 15 %. The alpha and beta are less sensitive to sorption mass, therefore the uncertainty of the optimized values is much higher. Except for the uncertainty of experimental sorption mass, the FE geometry could also affect the accuracy of optimized parameter values. Fig. 8(c) depicts the sorption results using two geometries with and without curved surface. The curved surface enables more areas directly exposed to vapor, faster sorption can thus be seen in the beginning. As shown in Fig. 8(d), the ellipsoid height of 1.3 mm ~ 1.7 mm has limited effect on the moisture sorption, while the sample of 40 ± 1 mg could cause 2.6 % sorption difference. To reduce the relative systematic errors, increase the repeatability of moisture sorption tests and obtain transport parameters with lower uncertainty, it is recommended to increase sample mass and have more replicate tests in follow-up studies.

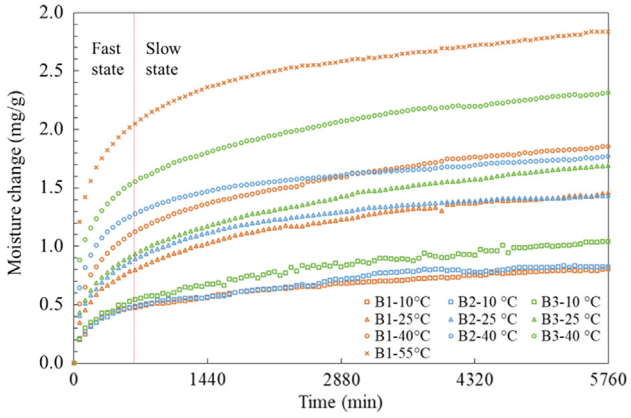

Fig. 9. Moisture sorption of bituminous binders at different temperatures and 80% relative humidity for four days (data is collected every second; in the graph the data points every 60 min are plotted).

3.2. Moisture transport behavior

3.2.1. Moisture transport at the relative humidity of 80 %

The experimental moisture sorption of three bituminous binders at multiple temperatures and 80 % relative humidity can be seen in Fig. 9. The fast sorption rate is appreciable at initial stage which is assumed to be combined surface adsorption and bulk absorption. At slow state, the mass increase rate (the slope at each point) decreases rapidly, where the surface adsorption is close to the equilibrium state and mass increase is mainly due to the bulk diffusion in bitumen. Equilibrium moisture sorption amount and sorption rate increase with temperature for all bitumen types. Three bitumen types display different transport behavior. Apparently, at the same temperature, the SBS-polymer modified bitumen (B3) shows much higher sorption amount than the base bitumen (B1 and B2), and B2 has a slightly faster sorption rate compared to B1.

The optimized parameter values of the Dual, S-Fick and S-Cluster models are listed in Tables 3, 4 and 5, respectively. The Dual model and S-Fick models decompose the overall sorption into two modes; the Dual model assumes both modes following Fick's law with different diffusion coefficients and the S-Fick model assumes one mode belonging to surface adsorption and the other mode to bulk absorption. Both models discern two transport types, one with faster transport rate and the other slower transport rate. Two transport types display higher sorption and faster transport rate with increasing temperature. The faster mode in the Dual model is approximately equivalent to the surface adsorption of S-Fick model from the perspective of sorption mass and sorption rate. One challenge here is to identify whether the faster transport mode belongs to surface adsorption as assumed by the S-Fick model or another bulk diffusion type. Many studies have discussed adsorption and absorption processes of water in organic materials [9,37]. Adsorption normally displays faster rate than absorption due to fewer barriers from the surrounding components. Considering that, in this work, water sorption is measured using water vapor, the faster transport mode can be assumed to be surface adsorption. In this regard, the surface adsorption rate is more than ten times faster than bulk absorption according to the parameter values of the Dual model.

For the S-Cluster model, when the Henry's absorption is lower than the cluster threshold c_H^0, the S-Cluster model is the same as the S-Fick model where fast surface adsorption dominates the water sorption at initial state. The bulk absorption in Henry's mode increases gradually with time, along with the generation of water cluster when the Henry's concentration is higher than c_H^0. The cluster absorption is dependent on the Henry's concentration, cluster size and cluster reaction rate. When the Henry's sites in bitumen are occupied, water molecules are primarily bound to polar sites of bitumen or to each other to form water cluster groups. Clusters have a larger volume size compared to a single water molecule. According to the free volume theory, diffusion requires sufficient spaces (free volume) with a certain size and enough energy for molecules to jump between adjacent spaces [38]. A commonly used equation to correlate penetrant size and diffusion coefficient for dilute solutions is [39]:

$$D = \gamma T M^{0.5}/(\eta d^{1.8}) \tag{18}$$

where γ is a constant dependent on system properties, M is the molecular weight of solvent, η denotes the viscosity of solvent and d is the molecular diameter of penetrant. From this equation, it can be inferred that two water molecules clustering together could lead to an approximately-four (4) times lower diffusion coefficient. Diffusion at higher temperature exhibits bigger cluster size (Table 5), which verifies again the abnormal diffusion coefficient change with temperature due to two counteracting factors, i.e. the temperature and the cluster size. The B1 and B2 binders display similar cluster size, which is larger than binder B3 at all temperatures. The smaller water cluster size in the SBS modified bitumen could be due to the internal structure of the bitumen-polymer systems limiting the formation of water clusters [40].

3.2.2. Moisture transport at multi-step relative humidity

Fig. 10 shows the isotherm results of B1 at three temperatures. A linear correlation between relative humidity and moisture content can be observed when relative humidity is smaller than 70 % $\sim$ 80 %. At high relative humidity, sorption isotherms deviate from the linear state, indicating a different water sorption mechanism. The overall sorption amount increases with temperature at nearly all the RH steps. As aformentioned, the S-Cluster model displays better performance at higher sorption amount, therefore the S-Cluster model was used to analyze multi-step sorption test results. The S-Cluster model was simplified into the S-Fick model at low RH steps when the Henry's concentration is lower than the cluster threshold. As depicted in Fig. 11, both surface adsorption and bulk absorption display approximately linear realtionship with relative humidity before ca. 70 % RH. At higher relative humidity, bulk water clustering occurs and the moisture soprtion amount increases rapidly with relative humidity, highlighting that cluster formation is the dominatint mechanism at this stage.

3.3. Moisture diffusion coefficient

3.3.1. Moisture diffusion coefficient at the relative humidity of 80 %

Diffusion is an activated process, thus diffusion coefficient increases with temperature. Studies [41] have shown that the diffusion coefficient dependence on temperature follows the Arrhenius equation:

$$D = D_0 \exp(-E_A/RT) \tag{19}$$

where D is the diffusion coefficient, D_0 is the maximal diffusion coefficient, E_A is the activation energy for diffusion, T is the temperature and R is the universal gas constant. The equation can be modified to a linear expression:

$$\ln D = \ln D_0 - \frac{E_A}{R}\frac{1}{T} \tag{20}$$

From Fig. 12(a) and (b), it can be observed that the diffusion coefficients obtained from the Dual model and the S-Fick model contradict the assumption of an Arrhenius-type temperature dependence of the diffusion coefficient. The diffusion coefficient at 25 °C is higher than other temperatures for the B1 and B2 binders. The S-Cluster model provides diffusion coefficient values that follow precisely the Arrhenius equation. According to the Equation (13) from the S-Cluster model, the real-time diffusion coefficient keeps constant in the beginning (before clustering threshold) and then decreases with increasing moisture concentration after clustering occurs. In contrast, the diffusion coefficients obtained from the S-Fick and Dual models could represent an average value over

Table 3
Optimized parameters of the Dual model at 80% RH and different temperatures (T).

Dual	T (°C)	c_1(mol/m^3)	c_2(mol/m^3)	D_1(m^2/s)	D_2(m^2/s)	Objective
B1	10	15.3	40.2	3.0E-11	9.2E-13	8.0E-06
	25	15.0	75.8	4.5E-11	1.6E-12	4.9E-06
	40	34.9	89.9	2.7E-11	1.0E-12	4.8E-06
	55	72.1	92.2	6.6E-11	2.3E-12	3.9E-05
B2	10	12.8	49.4	3.0E-11	7.6E-13	1.7E-05
	25	13.5	69.7	8.4E-11	2.9E-12	2.0E-06
	40	52.9	53.4	3.0E-11	1.6E-12	8.8E-06
B3	10	9.6	60.3	4.3E-11	1.1E-12	9.8E-06
	25	21.0	92.4	4.2E-11	1.1E-12	2.7E-06
	40	48.5	91.0	7.7E-11	1.8E-12	8.9E-06

Table 4
Optimized parameters of the S-Fick model at 80% RH and different temperatures (T).

S-Fick	T (°C)	D_{sf}(m^2/s)	α(1/s)	s_{m-sf}(kg)	c_{sat-sf}(mol/m^3)	Objective
B1	10	9.5E-13	0.012	9.0E-09	43.2	9.2E-06
	25	1.7E-12	0.015	9.7E-09	76.1	5.2E-06
	40	1.4E-12	0.011	2.1E-08	88.5	1.1E-05
	55	2.6E-12	0.022	4.7E-08	95.3	4.9E-05
B2	10	1.0E-12	0.012	7.8E-09	47.0	2.3E-05
	25	2.8E-12	0.018	1.0E-08	69.1	2.6E-06
	40	2.5E-12	0.013	3.0E-08	58.7	1.9E-05
B3	10	1.0E-12	0.012	6.6E-09	60.5	1.2E-05
	25	1.2E-12	0.014	1.4E-08	91.8	4.3E-06
	40	1.9E-12	0.023	3.3E-08	91.9	1.2E-05

Table 5
Optimized parameters of the S-Cluster model at 80% RH and different temperatures (T).

S-Cluster	T (°C)	D_{sc}(m^2/s)	α(1/s)	n	s_{m-sc}(kg)	β	c^0_H(mol/m^3)	c_{sat-sc}(mol/m^3)	Objective
B1	10	1.1E-12	0.010	1.13	5.9E-09	0.41	42.9	47.6	8.5E-06
	25	2.1E-12	0.017	1.28	8.8E-09	0.90	67.0	75.2	4.7E-06
	40	3.2E-12	0.017	1.68	1.5E-08	0.92	69.0	80.3	8.2E-06
	55	5.5E-12	0.030	1.90	3.9E-08	1.01	87.0	94.6	4.3E-06
B2	10	1.6E-12	0.010	1.32	8.3E-09	0.40	35.3	41.2	2.4E-05
	25	3.0E-12	0.014	1.42	1.1E-08	0.85	63.4	67.6	3.9E-06
	40	4.6E-12	0.015	1.52	2.6E-08	0.91	53.1	59.0	6.4E-06
B3	10	1.8E-12	0.010	1.03	5.4E-09	0.56	39.3	54.2	1.1E-05
	25	2.7E-12	0.016	1.26	1.2E-08	0.42	52.5	74.2	3.5E-06
	40	3.6E-12	0.036	1.31	2.8E-08	1.08	75.0	86.2	9.0E-06

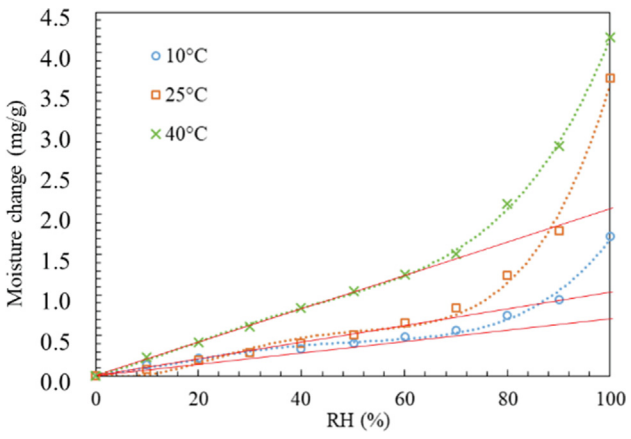

Fig. 10. Isotherm curves of B1 at different temperatures (i.e. 10 °C, 25 °C and 40 °C). The dotted lines are fitting results using 4-order polynomial and the red lines indicate the sorption before 70 % ~ 80 % RH when moisture content increases linearly with relative humidity. (For interpretation of the references to colour in this figure legend, the reader is referred to the web version of this article.)

the whole testing period. The S-Cluster model eliminates the effect of clustering and acquires the Henry's diffusion coefficient in dilute solution, thus showing typical increase with temperature. Fig. 12 depicts the regression results of three bitumen types. The activation energy of B1 and B2 is similar and higher than that of the B3 binder, which physically denotes a more difficult diffusive jump of water molecules. The activation energy is solely affected by the physiochemical and structural properties of bituminous binders. Hence, it is reasonable that the B1 and B2 binders with similar physical properties will show comparable activation energies. Adding polymers causes the formation of a polymer network in bitumen, which could change the hopping barriers for water molecules.

3.3.2. Effect of relative humidity on diffusion coefficient

The diffusion coefficient has been shown to decrease with increasing water concentration due to clustering and immobilization of water molecules through hydrogen bonding. According to the S-Cluster model, the diffusion coefficient is a function of the water cluster amount. A constant diffusion coefficient is expected before the clustering threshold, after which the diffusion coefficient shows a rapid decline with water cluster accumulation (Fig. 13(a)). For the multi-step sorption, the S-Cluster model was utilized to solve the transport kinetics at every RH step in the conditions of already existing moisture absorption from the previous RH step, therefore the derived diffusion coefficients show the Henry's diffusion rate affected by Henry's moisture concentration (Fig. 13(b)). A general decreasing trend of Henry's diffusion coefficient can be observed as the relative humidity increases (absorption increases), while this decline is much slower compared to the effect of clustering behavior (Fig. 13(a)). The diffusion coefficient of Henry's sorption is thus not exactly constant as the S-Cluster model assumes. However, neglecting the decrease with increasing Henry's concentration is acceptable considering the much more explicit clustering effect.

3.4. Thermodynamics of moisture transport

3.4.1. Isothermal surface adsorption and bulk absorption

According to the S-Fick and S-Cluster models, the overall moisture sorption is divided into surface adsorption and bulk absorption as shown in Fig. 14. The pronounced increase of sorption at 100 % RH and 25 °C in Fig. 10 can be assigned to high surface adsorption of moisture. The DVS equipment is calibrated at 25 °C, where almost 100 % RH can be generated. At higher temperature, however, the actual relative humidity in the sample chamber is 96 % ~ 97 % RH. For the saturated vapor partial pressure, there is a dynamic equilibrium between the exchange of liquid and vapor water. Therefore, even a small addition of water could

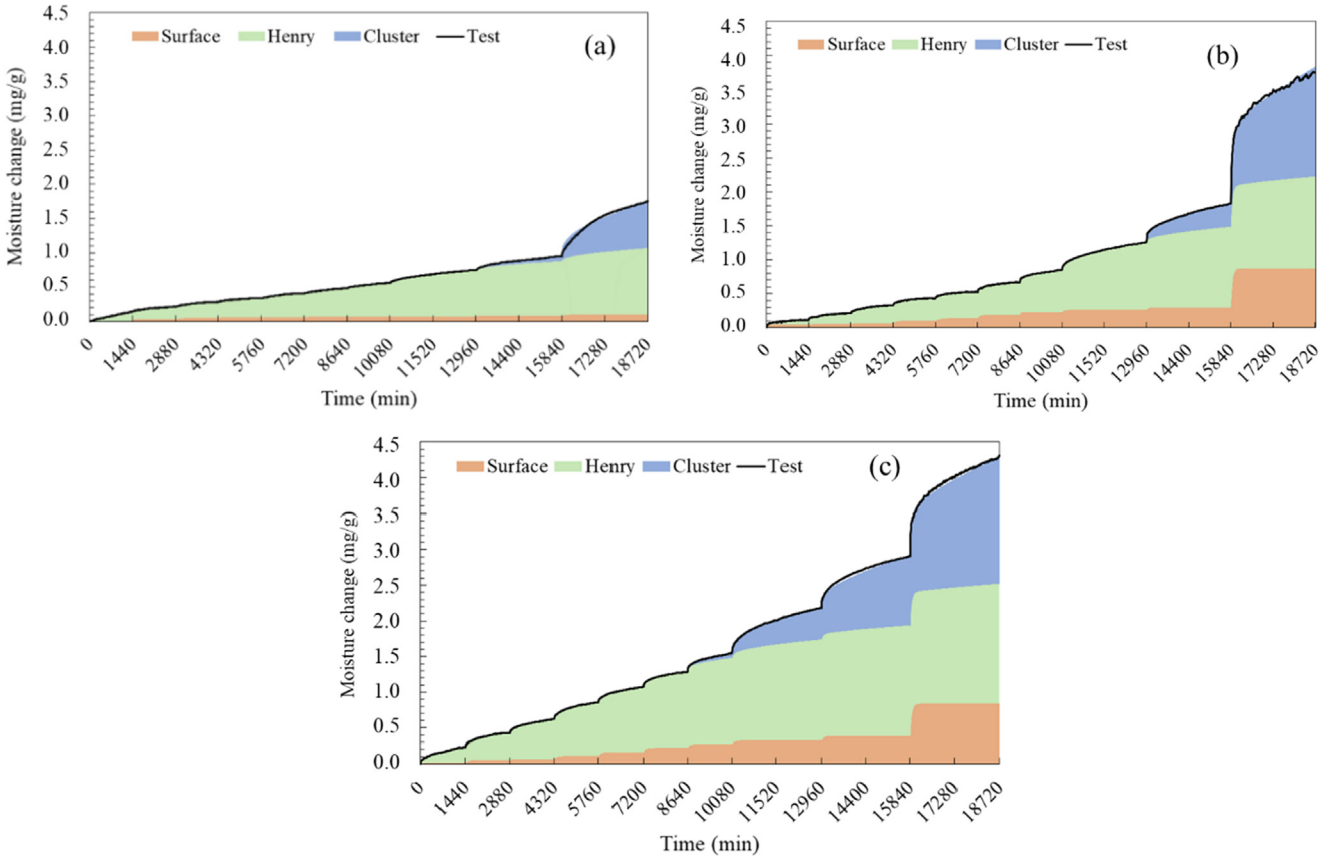

Fig. 11. Multi-step sorption tests and simulation results using the S-Cluster model of the B1 binder at temperatures of (a) 10 °C, (b) 25 °C and (c) 40 °C.

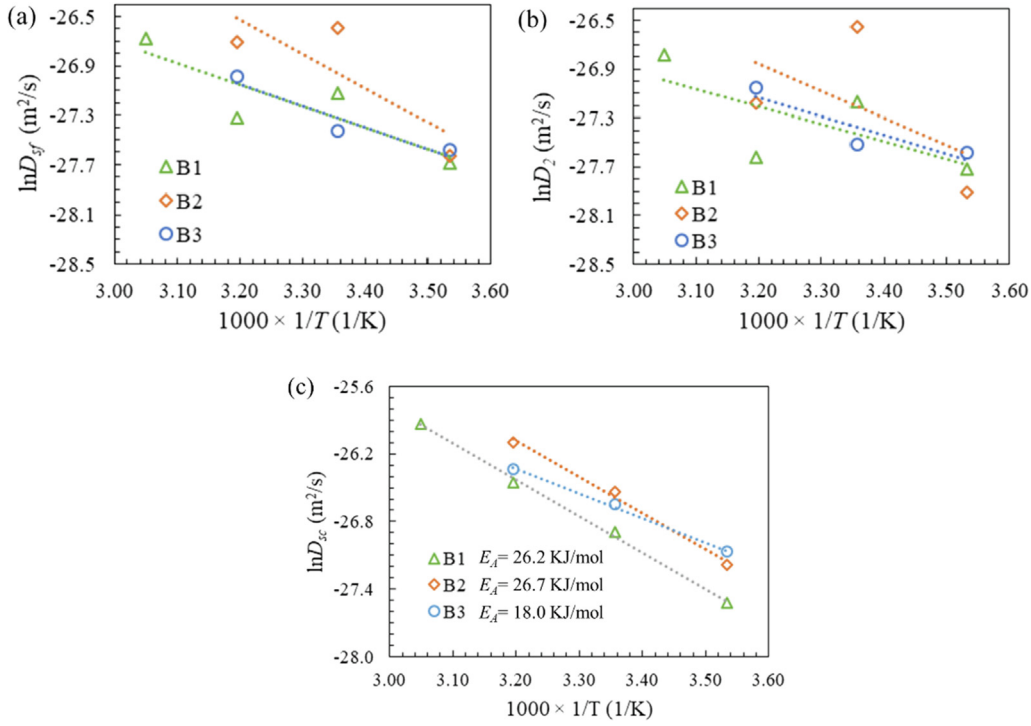

Fig. 12. Temperature dependence of diffusion coefficients obtained from the (a) S-Fick model, (b) Dual model and (c) S-Cluster model, where dotted lines are fitting results using the Arrhenius equation.

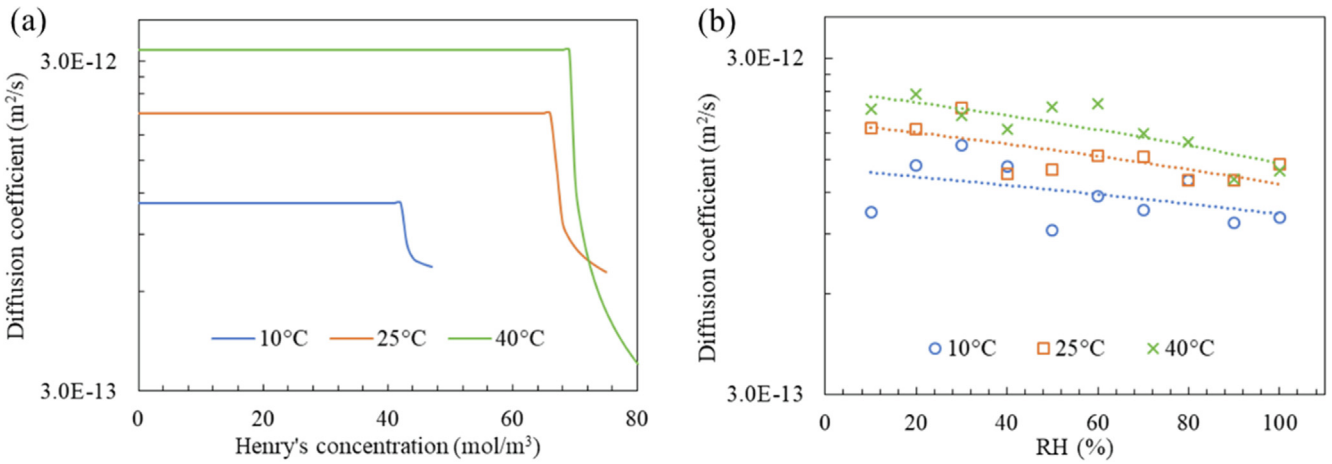

Fig. 13. Diffusion coefficient as a function of moisture concentration: (a) diffusion coefficient change with Henry's concentration according to the S-Cluster model; (b) diffusion coefficient (optimized using the S-Cluster model at each RH step from multi-step sorption results) at the various RH levels.

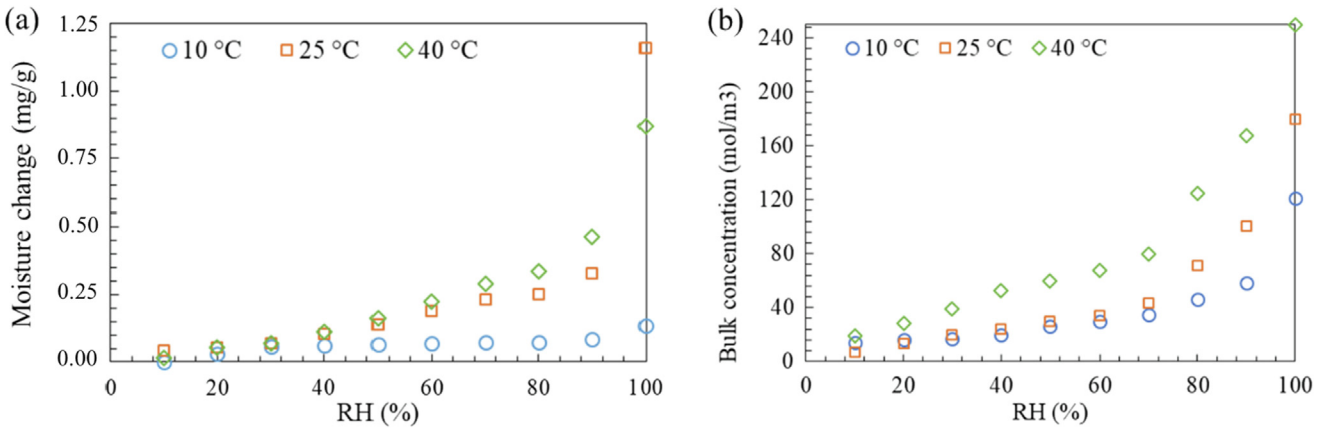

Fig. 14. Decomposed isotherm curves of B1 using the S-Cluster model: (a) surface adsorption, and (b) bulk absorption.

lead to vapor condensation, and as a result extremely high surface adsorption at 25 °C could be expected.

Two factors are responsible for surface adsorption, namely temperature and vapor partial pressure (relative humidity is the ratio of vapor partial pressure and saturated vapor partial pressure), which also increases with temperature. Physical adsorption of vapor to the solid surface is accompanied by a decrease in entropy and free energy of the system, and thus decreases with increasing temperature. On the other hand, surface adsorption increases with relative humidity (vapor partial pressure) at each temperature as revealed from the adsorption isotherm curves from Fig. 14(a). These two contracting factors are responsible for the adsorption isotherms changing with temperature illustrated in Fig. 14(a). The Clausius-Clapeyron equation [42] was used to describe the isosteric heat of sorption Q_{st}:

$$\frac{\partial \ln p}{\partial (1/T)} = \frac{Q_{st}}{R} \tag{21}$$

The isosteric heat of sorption as calculated from the three sorption isotherms is about −42.13 ∼ -35.85 kJ/mol, indicating an overall exothermic moisture sorption. The heat of condensation for water is −43.99 kJ/mol. The isosteric heat of sorption of the water surface adsorption is practically smaller than −43.99 kJ/mol taking into account the extra energy release due to the van der waals force interaction between water and adsorbate surface. The higher heat of sorption indicates a different sorption behavior with smaller energy release or even positive energy intake. The moisture concentration in Henry's mode is explained by Henry law, where the dependence of Henry' constant on temperature is regressed by the Arrhenius equation, as shown in Fig. 15. The enthalpy of dissolution for the three bitumen types is −33.9 ∼ -35.9 kJ/mol, agreeing with the heat of sorption values as calculated earlier using the Clausius-Clapeyron equation.

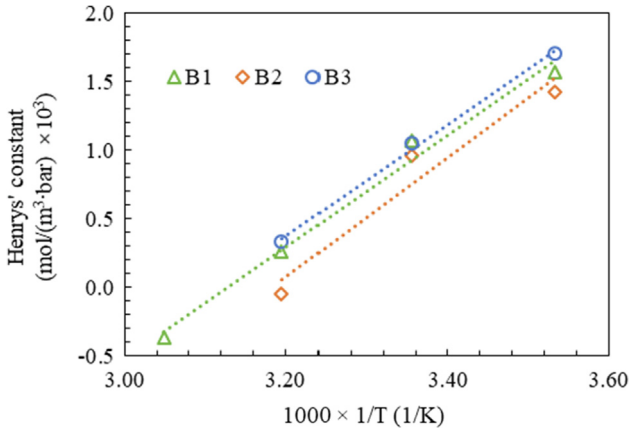

Fig. 15. The Henry's constant for the Henry's adsorption of water in bitumen at 80% RH.

3.4.2. Moisture solubility at low relative humidity

There are two stages in the absorption isotherms: a Henry stage for relative humidity ca. 0 ~ 70 % where a linear correlation exists between relative humidity and water absorption and a clustering stage with faster increase of absorption at higher relative humidity levels. The Flory-Huggins solution theory is a well-known lattice-based thermodynamic model of polymer solutions which considers the interaction between solvent and solute according to the following equation:

$$\ln a = \ln \phi_1 + (1 - \phi_1) + \chi(1 - \phi_1)^2 \tag{22}$$

where a is the water activity, ϕ_1 is the water volume fraction and χ in the interaction parameter. The theory shows good agreement with experimental results in semi-dilute concentration, while fails to describe the water absorption behavior at higher water activity (relative humidity) in some materials [43]. As the water cluster mechanism is not considered in the Flory-Huggins theory, the isotherm results from 0 to 70 % were used here to analyze the water-bitumen absorption and their interaction (χ), when no clustering occurs. Moreover, the interaction parameter can be derived from the Hansen solubility parameter as follows:

$$\chi = V_m(\delta_2 - \delta_1)^2/RT \tag{23}$$

where δ_1 and δ_2 are the solubility parameters of water and bitumen, respectively, and V_m is the molar volume of water. Regardless of the complex components, the solubility parameter of a Venezuelan bitumen was reported as 19.2 $MPa^{0.5}$ [44,45]. The solubility parameter of water at 25 °C is 47.8 $MPa^{0.5}$ [46]. As a result, an interaction parameter of 5.94 for water-bitumen systems is obtained from the Hansen solubility parameter. Fig. 16 depicts the isotherm curves fitted by Flurry-Huggins theory, where an interaction parameter of 5.79 is obtained at 25 °C, quite close to that derived from the Hansen solubility parameter. A higher interaction parameter physically demonstrates the immiscibility between water and bitumen. As temperature increases, the interaction parameter decreases, thus enhancing the miscibility of water in bitumen. The interaction parameter is a function of reciprocal temperature and related to free energy of the mixing process, which is not pronounced in Fig. 16 due to limited test temperatures. The similarity of the interaction parameter from the isotherm curves and the solubility parameter signifies a possibility to use water sorption tests as an indirect method to measure the solubility parameter of bituminous binders.

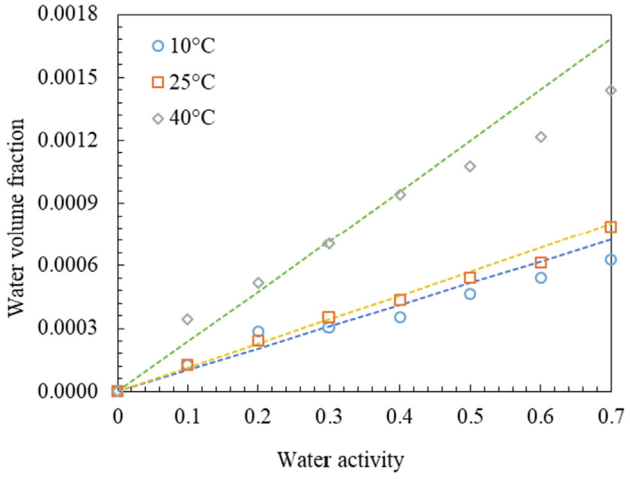

Fig. 16. Isotherm results (symbols) and Flory-Huggins model regression (dashed lines) at 10 °C, 25 °C and 40 °C.

3.4.3. Cluster at high relative humidity

Zimm and Lundberg [47] introduced a cluster integral parameter to illustrate the cluster tendency of water molecules in a polymer:

$$G_{11}/\upsilon_1 = -(1 - \phi_1)\left[\partial(\frac{\alpha_1}{\phi_1})/\partial\alpha_1\right]_{P,T} - 1 \tag{24}$$

where G_{11} is the cluster integral, υ_1 the partial molar volume of diffusing species, α_1 the water activity and ϕ_1 the water volume fraction. When G_{11}/υ_1 is smaller than -1, the water activity is linearly proportional to volume fraction, and gas or vapor molecules are more likely to stay isolated. WhenG_{11}/υ_1 > -1, the molecules start to cluster and thus exert more complex effect on the whole sorption and diffusion process. The mean number of water molecules in a cluster (water cluster size) is denoted by $\phi_1 G_{11}/\upsilon_1$ and is shown in Fig. 17(a). Bitumen, despite the existing polar groups from aromatics and asphaltenes, is a hydrophobic material lacking hydrogen bonding sites. Water molecules can have three states in bitumen: free state, bound to polar sites, and water clusters. In the case that the affinity between water and bitumen is much lower than the affinity of water molecules themselves, water molecules tend to cluster via hydrogen bonding. Due to the low solubility of free water and the lack of polar sites, the water cluster behavior is expected at higher relative humidity. Water cluster probably occurs firstly among polar sites and grows using these sites as nucleus as illustrated in Fig. 17(b).

4. Conclusions

Water transport in bitumen is one of the critical mechanisms responsible for moisture damage in asphalt pavements. It is therefore of great importance to understand the water transport behavior at various temperatures and relative humidity levels. To study the moisture transport kinetics and thermodynamics in bitumen, three moisture transport models were utilized and compared. The effect of bitumen type, temperature and relative humidity on the moisture transport behavior, especially the diffusion coefficient, solubility and cluster mechanisms were quantified and evaluated.

The three models show a great overall quality of simulating the experimental results. The S-Cluster model, however, have proven to be more appropriate at higher sorption levels, compared with the S-Fick model and Dual models. The S-Cluster model reveals that the bulk absorption mechanisms comprises the Henry's diffusion with constant diffusion coefficient and the water cluster mechanisms. The Henry's diffusion coefficient follows precisely the Arrhenius equation. At high moisture concentration levels, water molecules could cluster together to form big droplets and significantly decrease the moisture transport rate. In practice, the S-Fick model and Dual models are recommended for simple modeling and parameter determination considering the limited unknown parameters. The S-Cluster model is highly recommended when studying water transport at higher temperature and relative humidity levels, at which high moisture sorption is expected, and when a more detailed explanation of water transport mechanisms is required.

The studied bitumen types possess different transport behavior at the relative humidity of 80 %. Compared to the base bitumen, the polymer modified bitumen has shown smaller water cluster sizes, lower diffusion activation energy and higher sorption. These properties could be linked to the structure changes and polymer network formation after adding the polymers. The two base bitumen types also display differences in their diffusion coefficient and solubility, although they have the same penetration grade. A faster diffusion coefficient seems to be accompanied by a lower solubility

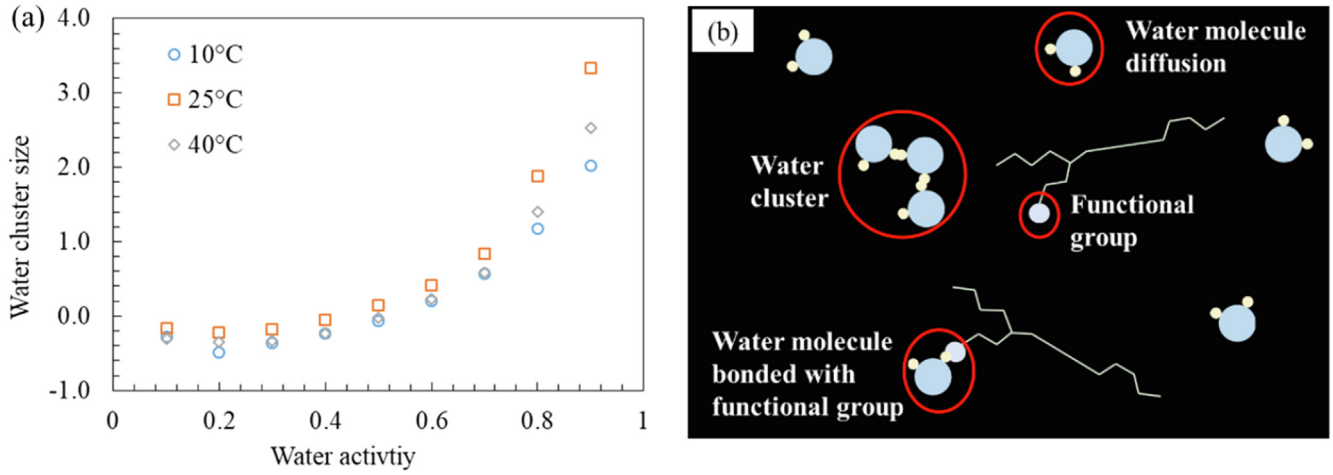

Fig. 17. (a) Evolution of mean water cluster size with water activity for the B1 binder determined by the Zimm-Lundberg model, (b) water transport and clustering mechanisms in bitumen.

for the base bitumen. The effect of temperature of the moisture sorption is quantified by the Clausius-Clapeyron equation. Both surface adsorption and Henry's solubility are proved to be exothermic processes. The overall sorption change with temperature is dominated by the decrease of sorption at certain vapor partial pressure and the increase of vapor partial pressure with increasing temperature. At high relative humidity of 70 % ~ 100 %, the moisture sorption increases much faster than at low relative humidity, suggesting the occurrence of water clusters. To study the interaction between moisture and bitumen, at low relative humidity, the Flurry-Huggins theory was applied. The derived interaction parameter is close to the value obtained from the Hansen solubility parameter of water and bitumen, revealing a feasible method to measure the Hansen solubility parameter of various bituminous binders via moisture sorption tests. The cluster behavior at high relative humidity is also verified by the Zimm-Lundberg model. As a result, moisture in bitumen is firstly present as free state with constant (or slightly decreasing with Henry's concentration) diffusion coefficient, and then bonded to polar sites of bitumen or clusters together to form droplets via hydrogen bonding, accompanied by a quick drop of the moisture diffusion coefficient.

The diffusion coefficient, activation energy, cluster size etc. depend on bitumen properties such as free volume, viscosity, bitumen components, bitumen-polymer structures, ageing conditions. Further study will be focused on the correlation between transport parameters and bitumen properties, especially for bitumen at various ageing states.

Data availability

Data will be made available on request.

Declaration of Competing Interest

The authors declare that they have no known competing financial interests or personal relationships that could have appeared to influence the work reported in this paper.

Acknowledgements

This publication is part of the project 'A multiscale approach towards future road infrastructure: How to design sustainable paving materials?' (with project number 18148) of the research programme NWO Talent Programme Veni AES 2020 which is financed by the Dutch Research Council (NWO). This work was also partly funded by the China Scholarship Council (CSC). The authors would like to thank Ms. Xiuli Wang from Delft University of Technology for her valuable help in performing the microscope measurements.

References

[1] Z. Chen, H. Zhang, H. Duan, Investigation of ultraviolet radiation aging gradient in asphalt binder, Constr. Build. Mater. 246 (2020) 118501.
[2] M. Nobakht, D. Zhang, M.S. Sakhaeifar, R.L. Lytton, Characterization of the adhesive and cohesive moisture damage for asphalt concrete, Constr. Build. Mater. 247 (2020) 118616.
[3] A.R. Copeland, J. Youtcheff, A. Shenoy, Moisture sensitivity of modified asphalt binders, Transp. Res. Record: J. Transp. Res. Board 1998 (1) (2007) 18–28.
[4] Y. Yuan, X. Zhu, L. Chen, Relationship among cohesion, adhesion, and bond strength: from multi-scale investigation of asphalt-based composites subjected to laboratory-simulated aging, Mater. Des. 185 (2020) 108272.
[5] C.A. Lemarchand, M.L. Greenfield, J.S. Hansen, Dynamics and structure of bitumen-water mixtures, J Phys Chem B 120 (24) (2016) 5470–5480.
[6] K. Kanitpong, Evaluation of the Roles of Adhesion and Cohesion Properties of Asphalt Binders in Moisture Damage of HMA, University of Wisconsin-Madison, 2004.
[7] A.K. Apeagyei, J.R.A. Grenfell, G.D. Airey, Moisture-induced strength degradation of aggregate-asphalt mastic bonds, Road Mater Pavement 15 (sup1) (2014) 239–262.
[8] N. Kringos, A. Scarpas, Physical and mechanical moisture susceptibility of asphaltic mixtures, Int J Solids Struct 45 (9) (2008) 2671–2685.
[9] D. Cheng, D.N. Little, R.L. Lytton, J.C. Holste, Moisture damage evaluation of asphalt mixtures by considering both moisture diffusion and repeated-load conditions, Transp. Res. Rec. 1832 (1) (2003) 42–49.
[10] T. Ogawa, T. Nagata, Y. Hamada, Determination of diffusion coefficient of water in polymer films by TGA, J Appl Polym Sci 50 (1993) 981–987.
[11] K.L. Vasconcelos, A. Bhasin, D.N. Little, Measurement of water diffusion in asphalt binders using Fourier transform infrared-attenuated total reflectance, Transp. Res. Record 2179 (1) (2010) 29–38.
[12] C. Maggana, P. Pissis, Water sorption and diffusion studies in an epoxy resin system, J. Polym. Sci. Pol. Phys. 37 (11) (1999) 1165–1182.
[13] A.A. Apeagyei, G.D. Airey, J.R.A. Grenfell, Application of Fickian and non-Fickian diffusion models to study moisture diffusion in asphalt mastics, Mater. Struct. 48 (5) (2015) 1461–1474.
[14] H.N. Xu, J. Zhou, Q.F. Dong, Y.Q. Tan, Characterization of moisture vapor diffusion in fine aggregate mixtures using Fickian and non-Fickian models, Mater. Des. 124 (2017) 108–120.
[15] P.R. Herrington, J.P. Wu, L.C. van den Kerkhof, S.A. Bagshaw, Water diffusion in bitumen films, Constr. Build. Mater. 294 (2021) 123530.
[16] S. Azizian, Kinetic models of sorption: a theoretical analysis, J. Colloid Interf. Sci. 276 (1) (2004) 47–52.
[17] K.Y. Foo, B.H. Hameed, Insights into the modeling of adsorption isotherm systems, Chem. Eng. J. 156 (1) (2010) 2–10.
[18] C. Yang, X. Xing, Z. Li, S. Zhang, A comprehensive review on water diffusion in polymers focusing on the polymer-metal interface combination, Polymers (Basel) 12 (1) (2020) 138.
[19] Z.Y. Liu, L.P. Cao, T. Zhou, Z.J. Dong, Multiscale investigation of moisture-induced structural evolution in asphalt-aggregate interfaces and analysis of

the relevant chemical relationship using atomic force microscopy and molecular dynamics, Energ. Fuel 34 (4) (2020) 4006–4016.
[20] S.J. Metz, N.F.A. van der Vegt, M.H.V. Mulder, M. Wessling, Thermodynamics of water vapor sorption in poly(ethylene oxide) poly(butylene terephthalate) block copolymers, J. Phys. Chem. B 107 (49) (2003) 13629–13635.
[21] K.L. Vasconcelos, A. Bhasin, D.N. Little, History dependence of water diffusion in asphalt binders, Int. J. Pavement Eng. 12 (5) (2011) 497–506.
[22] L. Ma, A. Varveri, R. Jing, S. Erkens, Comprehensive review on the transport and reaction of oxygen and moisture towards coupled oxidative ageing and moisture damage of bitumen, Constr. Build. Mater. 283 (2021) 122632.
[23] Z. Cheng, F. Kong, X. Zhang, Application of the Langmuir-type diffusion model to study moisture diffusion into asphalt films, Constr. Build. Mater. 268 (2021) 121192.
[24] F. Gritti, G. Guiochon, Effect of the flow rate on the measurement of adsorption data by dynamic frontal analysis, J. Chromatogr. A 1069 (1) (2005) 31–42.
[25] E. Arthur, M. Tuller, P. Moldrup, L.W.d. Jonge, Evaluation of a fully automated analyzer for rapid measurement of water vapor sorption isotherms for applications in soil science, Soil Sci. Soc. Am. J. (78) (2014) 754–760.
[26] S.J. Harley, E.A. Glascoe, R.S. Maxwell, Thermodynamic study on dynamic water vapor sorption in Sylgard-184, J. Phys. Chem. B 116 (48) (2012) 14183–14190.
[27] A.W. Adamson, A.P. Gast, Physical Chemistry of Surfaces, John Wiley & Sons Inc, New York, 1997.
[28] R.B. Bird, W.E. Stewart, E.N. Lightfoot, Transport Phenomena, Wiley, New York, 2002.
[29] Y.S. Ho, G. Mckay, kinetic models for the sorption of dye from aqueous solution by wood, Trans. Inst. Chem. Eng. 96 (1998) 183–191.
[30] Y. Sun, S.J. Harley, E.A. Glascoe, Modeling and uncertainty quantification of vapor sorption and diffusion in heterogeneous polymers, ChemPhysChem 16 (14) (2015) 3072–3083.
[31] J. Crank, G.S. Park, Diffusion in Polymers, Academic Press, London, 1968.
[32] W.R. Vieth, J.M. Howell, J.H. Hsieh, Dual sorption theory, J. Membrane Sci. 1 (1976) 177–220.
[33] G.S. Park, Transport principles: solution, diffusion and permeation in polymer membranes, Synthetic Membranes: Science, Engineering and Applications, Dorcrecht, The Netherlands, 1986, p. 94.
[34] M.J.D. Powell, The BOBYQA Algorithm for Bound Constrained Optimization Without Derivatives, University of Cambridge, 2009.
[35] O. Harel, The estimation of R2 and adjusted R2 in incomplete data sets using multiple imputation, J. Appl. Statistics 36 (10) (2009) 1109–1118.
[36] D.G. Cacuci, M. Ionescu-Bujo, I.M. Navon, Sensitivity and uncertainty analysis, volume II: applications to large-scale systems, CRC Press, 2005.
[37] G.K. van der Wel, O.C.G. Adan, Moisture in organic coatings - a review, Prog. Org. Coat. 37 (1-2) (1999) 1–14.
[38] G. Bouvet, N. Dang, S. Cohendoz, X. Feaugas, S. Mallarino, S. Touzain, Impact of polar groups concentration and free volume on water sorption in model epoxy free films and coatings, Prog. Org. Coat. 96 (2016) 32–41.
[39] C.R. Wilke, P. Chang, Correlation of diffusion coefficients in dilute solutions, Am. Inst. Chem. Eng. 1 (2) (1955) 264–270.
[40] B. Sengoz, A. Topal, G. Isikyakar, Morphology and image analysis of polymer modified bitumens, Constr. Build. Mater. 23 (5) (2009) 1986–1992.
[41] P. Neogi, Diffusion in Polymers, New York, 1996.
[42] S. Poyet, S. Charles, Temperature dependence of the sorption isotherms of cement-based materials: Heat of sorption and Clausius-Clapeyron formula, Cem. Concr. Res. 39 (11) (2009) 1060–1067.
[43] J. Huang, I. Derue, P.Y. Le Gac, E.J.P.D. Richaud, Stability, Thermal oxidation of polydicyclopentadiene-Changes in water absorption, 180 (2020) 109219.
[44] P. Redelius, Bitumen solubility model using Hansen solubility parameter, Energ Fuel 18 (4) (2004) 1087–1092.
[45] J. Zhu, R. Balieu, H. Wang, The use of solubility parameters and free energy theory for phase behaviour of polymer-modified bitumen: a review, Road Mater Pavement 22 (4) (2021) 757–778.
[46] C.M. Hansen, Hansen Solubility Parameters: A User's Handbook, Taylor & Francis, Boca Raton, 2007.
[47] B.H. Zimm, J.L. Lundberg, Sorption of vapors by high polymers, J. Phys. Chem. 60 (4) (1956) 425–428.